NUCL SCI TECH (2018) 29:91
https://doi.org/10.1007/s41365-018-0419-8

2.856 GHz microwave signal extraction from mode-locked Er-fiber lasers with sub-100 femtosecond timing jitter

Wen-Yan Zhang[1] · Xiao-Qing Liu[1] · Lie Feng[1] · Tai-He Lan[1] · Xing-Tao Wang[1] · Bo Liu[1]

Received: 11 July 2017 / Revised: 16 November 2017 / Accepted: 27 November 2017 / Published online: 12 May 2018

Abstract A balanced optical microwave phase detector (BOMPD) based on a 3 × 3 coupler is presented. This system was developed to extract ultra-low-jitter microwave signals from optical pulse trains emitted by mode-locked Er-fiber lasers, and synchronized microwave and laser systems. We demonstrate that the BOMPD achieves a precision of synchronization of less than 100 femtosecond of timing jitter. The experimental setup can be applied to the soft X-ray free-electron laser located on the campus of the Shanghai synchrotron radiation facility. A microwave signal with a 2.856 GHz frequency is extracted from a 238 MHz mode-locked Er-laser, with an absolute timing jitter of 34 fs in the 10 Hz–10 MHz frequency offset range. In addition, the microwave and 238 MHz optical pulse signals are synchronized with a relative timing jitter of 16 fs at the same frequency offset range.

Keywords BOMPD · 3 × 3 coupler · Timing jitter · Mode-locked Er-fiber laser · SXFEL

This work was supported by the National Natural Science Foundation of China (No. 11175241).

✉ Xiao-Qing Liu
liuxiaoqing@sinap.ac.cn

✉ Bo Liu
liubo@sinap.ac.cn

1 Shanghai Institute of Applied Physics, Chinese Academy of Sciences, 239 Zhangheng Road, Pudong District 201800, Shanghai, China

1 Introduction

The X-ray free-electron laser (XFEL) [1–4], a next-generation light source, is considered to be a powerful scientific instrument, which will likely foreshadow unprecedented breakthroughs in multiple disciplines, and is arguably the most promising light source for the next generation of scientific exploration and discovery. Pump-probe experiments at the XFEL, with its excellent spatial and temporal resolution, can facilitate the observation of atomic scale microscopic phenomena that are of great significance to the development of biology, chemistry, material science, atomic and molecular physics and other fields [5–11]. The timing jitter between the pump laser pulses and the accelerator-based X-ray sources is the main limiting factor that influences the temporal resolution of X-ray pump-probe experiments [12–14]. At present, the critical task in these pump-probe experiments is to synchronize various pulsed lasers and microwave sources across hundreds of meters to multi-kilometer distances. The first XFEL's facility in China, i.e., the soft X-ray free-electron laser (SXFEL) is being constructed on the campus of the Shanghai synchrotron radiation facility [15]. Sub-100 femtosecond (fs) synchronization between the optical and RF sources can meet the demands of the SXFEL facility (see Fig. 1).

Low-jitter microwave signals are of great concern in the development of the SXFEL. Mode-locked Er-fiber lasers with fs-level pulse duration have been utilized to extract microwave signals that satisfy the requirement of SXFEL [16]. As has been shown recently, optical pulse trains with sub-femtosecond timing jitter can be emitted by mode-locked Er-fiber lasers that lock to a RF reference source [17–19].

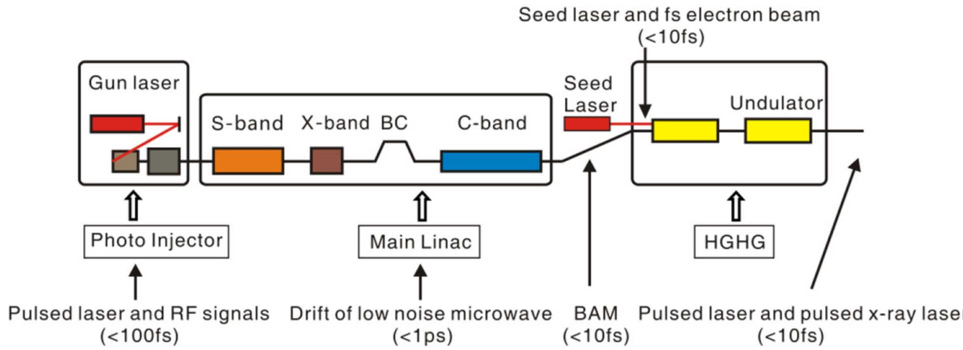

Fig. 1 (Color online) Technical parameters of the femtosecond timing system of SXFEL

There are three different methods to implement the synchrotron of optical and microwave signals, and include direct detection using a photodiode, microwave phase detection and BOMPD [20]. Direct detection achieves a high harmonic frequency of laser pulse signals by means of a photodetector and filter. However, excess noise is introduced by amplitude-to-phase conversion, temperature drift, beam-pointing variations and photodetector nonlinearities [21]. Therefore, this approach can only be used for applications that do not require high precision. Compared to the direct photodetection method, the synchronization accuracy of microwave phase detector can approach 200 fs. Microwave phase detection is a radio frequency synchronization technique based on mixers that are used as a phase detector. Thus, this method can introduce more phase noise, and the synchronization precision is limited by the high-frequency noise of the voltage-controlled oscillator (VCO) used in the approach. BOMPD is an optical synchronization method based on the Sagnac loop and balanced detection technique. This approach and fiber gyroscopes have similar operation principles [21, 22]. BOMPD is used as a phase detector, which comprises a Sagnac loop, a phase modulator and a 2×2 coupler. The 2×2 coupler is used in BOMPD that has been shown recently and it has been established to form a Sagnac loop for phase detection. More details on the principle, physical design and technical parameters of the BOMPD can be seen in published reports [23, 24]. Compared to direct photodetection and microwave phase detection, BOMPD based on a 2×2 coupler is a synchronization detector that is not affected by detector nonlinearities and amplitude-to-phase conversion. A $\pi/2$ phase shift scheme is needed in such a system because of the phase properties at the output ends of the 2×2 coupler. The synchronization precision of BOMPD is less than 10 fs.

To improve the synchronization precision of optical–RF systems, we have developed a novel synchronization scheme. A BOMPD based on a 3×3 coupler is used for the suppression of excess noise, and any other nonreciprocal component is no longer necessary owing to the inherent characteristics of the 3×3 coupler [25]. When a microwave signal is locked to one mode-locked laser, the BOMPD device using a 3×3 coupler can achieve better synchronization performance. This scheme can be used for the femtosecond timing system of the SXFEL in addition to SDUV-FEL and other all high brightness electron devices based on the photo-injector, such as ultrafast electron diffraction (UED), Thomson scattering X-ray source and linear collider [26].

2 Principles and experiments

2.1 Operation principle

Figure 2 shows the principle diagram of the BOMPD based on a 3×3 coupler. An optical pulse signal and a microwave signal are synchronized using a phase-locked loop (PLL) with a BOMPD based on the 3×3 coupler as its phase detector.

The optical pulse signal is generated by a mode-locked laser with a repetition frequency f_R, which is split into three beams by the coupler. Then the input optical pulse signal is sent into the Sagnac loop in which a phase modulator is positioned. The two output pulses (port 1 and port 2) from the 3×3 coupler propagate in the Sagnac loop in the opposite direction. The output pulses of the Sagnac loop are detected by a balanced detector that directly acquires a difference signal ΔV for the two pulses. According to the operation principle of the phase modulator and Sagnac loop, ΔV is associated with the phase error $\Delta\theta$ between the

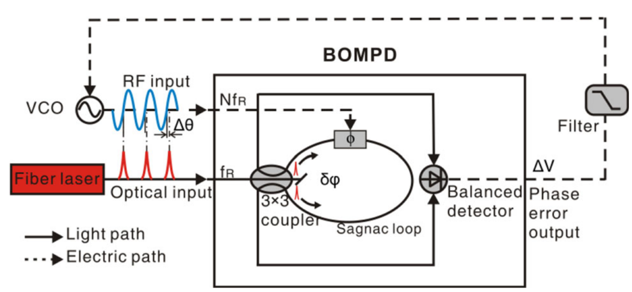

Fig. 2 A schematic of BOMPD based on 3×3 coupler

extracted microwave and the input optical signal. When $\sin\Delta\theta \approx \Delta\theta$, the difference signal is proportional to the phase error, that is $\Delta V = K_{PD} \cdot \Delta\theta$, where K_{PD} is the phase sensitivity in units of Volts/rad. The output voltage from the balanced detector is then transferred to a loop filter. The output of the loop filter is used as the control voltage of a VCO, which could change the VCO center frequency so that the phase error between the input optical signal and the VCO output is adjusted. The VCO output is then fed back to the phase modulator to form a closed loop. When the VCO's frequency is equal to Nf_R (N is a natural number), it locks on to the fiber laser. The phase error is constant when the PLL is in a locked state.

A BOMPD based on a 3 × 3 coupler includes a 3 × 3 coupler, a Sagnac loop, a high-speed $LiNbO_3$ phase modulator and a balanced detector (see Fig. 2). To lock the extracted microwave signal to the optical pulse train, a BOMPD based on a 2 × 2 coupler requires a π/2 phase shift bias in the Sagnac loop. However, this is not necessary for our BOMPD because of the inherent nonreciprocal performance of a 3 × 3 coupler. The input and output paths of the 3 × 3 coupler are different in the Sagnac loop, i.e., the smaller the output noise, the less the jitter of BOMPD. There is a fixed relationship between the phase and the output voltage of the three output ports of the 3 × 3 coupler, as shown in Fig. 3 [22]. Ideally, the outputs of port 1 and 2 at zero phase have equal amplitude and opposite slope. The Sagnac phase is determined by the difference signal of the two output optical pulses, without additional modulation in the loop. A BOMPD based on a 3 × 3 coupler is simple in structure and has fewer RF components. Therefore, this method could effectively eliminate the noise-based bottleneck problem associated with a BOMPD based on a 2 × 2 coupler. As a consequence, the BOMPD based on 3 × 3 coupler could extract higher precision microwave signals from the optical pulse trains.

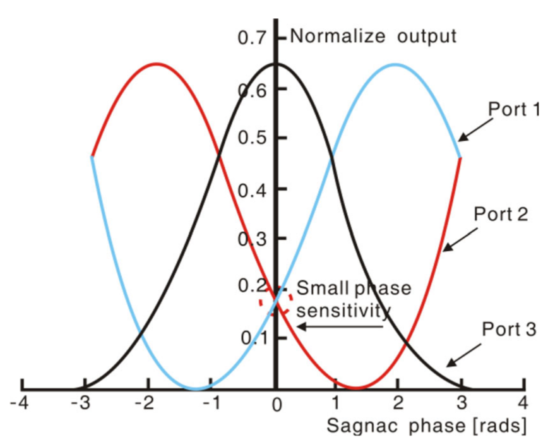

Fig. 3 (Color online) The outputs from ports 1, 2, 3 of 3 × 3 coupler as a function of Sagnac phase

2.2 Experimental setup

Figure 4 shows a schematic of the 2.856 G Hz microwave signal extraction system based on BOMPD. The optical reference signal is emitted by a mode-locked Er-fiber laser (Origami-15, Onefive GmbH), which operates at a 1550-nm center wavelength with an average output power of approximately 114 mW and a 150 fs pulse width. The fiber laser that has a repetition rate of 238 MHz is locked to a low-noise RF source to achieve long-term stability. The optical pulse signal generated from the fiber laser is sent to the BOMPD via a standard single-mode fiber (SMF, $D_2 \approx$ 20 ps/km/nm) and a specific length of dispersion compensating fiber (DCF, $D_2 \approx -$ 143 ps/km/nm). The DCF is inserted after the SMF to compensate for temporal stretching of the optical pulse caused by dispersion in the SMF and other optical devices. Then the compressed optical pulse is sent to the fiber Sagnac interferometer after passing through an isolator and a circulator in succession. The isolator is employed to prevent the input optical pulse train from reflecting into the fiber laser, while the circulator is established to provide an auxiliary monitor port. The fiber Sagnac interferometer is composed of a 3 × 3 coupler, a Sagnac loop and a 10 GHz $LiNbO_3$ phase modulator (PM-150-080, JDSU). There are three input ports and three output ports in the 3 × 3 coupler. Output port 1 is connected to the optical input of the phase modulator and output port 2 is connected to the optical output of phase modulator, so that a Sagnac loop is formed. As such, output port 3 is reserved as a monitor port while input port 3 is connected to the output port of the circulator. The two counter-propagating optical signals in the Sagnac loop are unidirectionally phase modulated by an external RF signal applied at the RF port of the $LiNbO_3$ phase modulator. Then the two optical signals are transmitted through the 3 × 3 coupler's input port 1 and input port 2. Subsequently, the outputs from the 3 × 3 coupler's input port 1 and input port 2 are transferred into a balanced detector (PDB450C, Thorlabs) for detecting the phase error between the two optical signals.

The phase error is transferred to a loop electronics PCB designed for appropriate filtering and amplification (see Fig. 4). A variable gain amplifier and a proportional–integral loop filter are employed to adjust the loop bandwidth to optimum the relative jitter. An additional two-order lead-lag filter is arranged before the VCO (CRO2856A-LF, Z-Communication) to further minimize the absolute jitter of the extracted microwave signal. The loop electronics PCB adopts low-noise electronic components to ensure excellent noise performance. The VCO with a 70 MHz

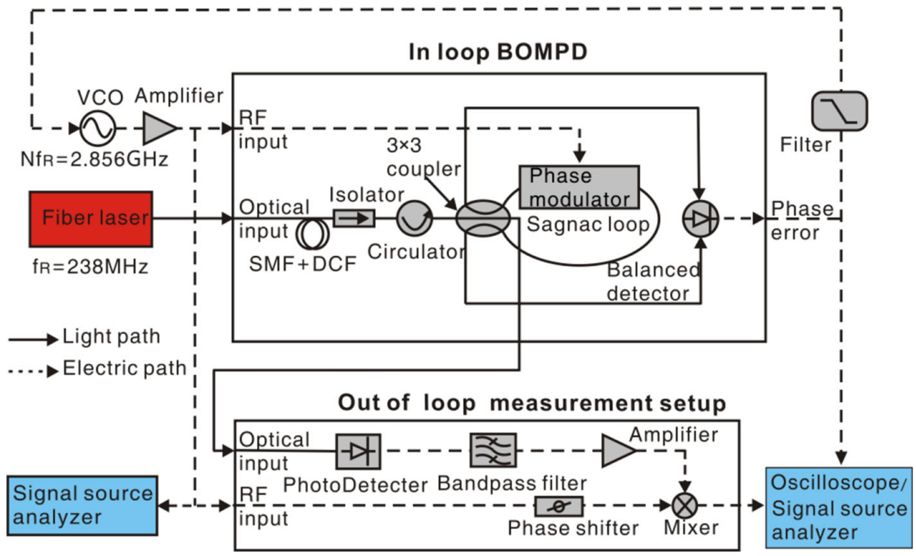

Fig. 4 Experiment setup for the 2.856 GHz microwave signal extraction system based on BOMPD and the out-of-loop measurement setup

tunable frequency range and a 7 MHz/V tuning sensitivity are also integrated into the loop electronics PCB. This ensures that an appropriate DC voltage bias is provided to maintain the VCO frequency at approximately 2.856 GHz, which is the 12th harmonic of the pulse train repetition rate. The VCO output is applied to the RF port of the aforementioned $LiNbO_3$ phase modulator for optical phase modulation. To achieve the high half-wave voltage $V\pi$ of the $LiNbO_3$ phase modulator, a low-noise amplifier (ZX05-33LN+, Mini-circuits) is deployed to amplify the VCO output signal to an appropriate average power at +13 dBm. Then the amplified VCO signal is fed back into the RF port of the phase modulator. The average input optical power is 20 mW, which further degrades the BOMPD's noise floor.

When the PLL is closed, the phase error from the BOMPD is appropriately handled by the loop electronics and then sent to the VCO tune voltage port to change the VCO instantaneous oscillation frequency. The phase of the optical pulse during propagation in the Sagnac loop can be influenced by the driving frequency of the phase modulator microwave. The VCO frequency is continually adjusted by the processed phase error signal until the optical pulse coincides with the zero-crossing point of the microwave driving signal of the phase modulator. Then the average input optical power sent to the balanced phase detector will be balanced, and the PLL is locked. In order to measure the relative jitter between the extracted microwave signal and the input optical signal when the PLL is locked, an out-of-loop measurement setup is also implemented (see Fig. 4). The monitor port output of the 3 × 3 coupler is detected by a photodetector (XPDV2120R-VF-FP, u^2t), then transmitted through a bandpass filter (BPF), then amplified by a high-gain and low-phase-noise amplifier (AFS27002900-06-13, Miteq) at 16 dBm average power. Finally the amplified signal is added to the LO port of a balanced frequency mixer (ZEM4300-MH+, Mini-circuits) of which the RF port is driven by the VCO signal. A phase shifter (D3448B, ARRA) is used to adjust the VCO signal's phase so that the phases of the VCO signal and the monitor signal from the 3 × 3 coupler are orthogonal in the mixer. The mixer's IF port is connected to a signal source analyzer (E5052B, Agilent) for base-band measurements to calculate the relative jitter between the extracted microwave signal and the input optical pulse. The extracted microwave signal's absolute jitter can be measured and evaluated by the signal source analyzer directly.

2.3 Short-term timing jitter measurement

Short-term stability measurement results are shown in Fig. 5. Figure 5(top) depicts the single-sideband (SSB) phase noise curves at the 2.856 GHz carrier in the 10 Hz–10 MHz frequency offset range. The free-running VCO phase noise (see green line) is obtained via a test board (MINIEVAL, Z-Communication). When the loop is closed, the phase error signal from the in-loop BOMPD (see Fig. 4) changes from a sine signal into a DC signal. This phenomenon that was observed using an oscilloscope indicated that the PLL was locked.

When the PLL is locked, the timing jitters of the in-the-loop and out-of-loop measurements are represented by a blue line and red line, respectively. The locked VCO phase noise is obtained via in-loop measurement setup. The relative jitter phase noise is obtained via out-of-loop measurement setup. The noise floor of the out-of-loop setup is represented by the orange line. This noise floor measurement setup includes an RF reference source, a power divider, a phase shifter, a mixer and the E5052B. The

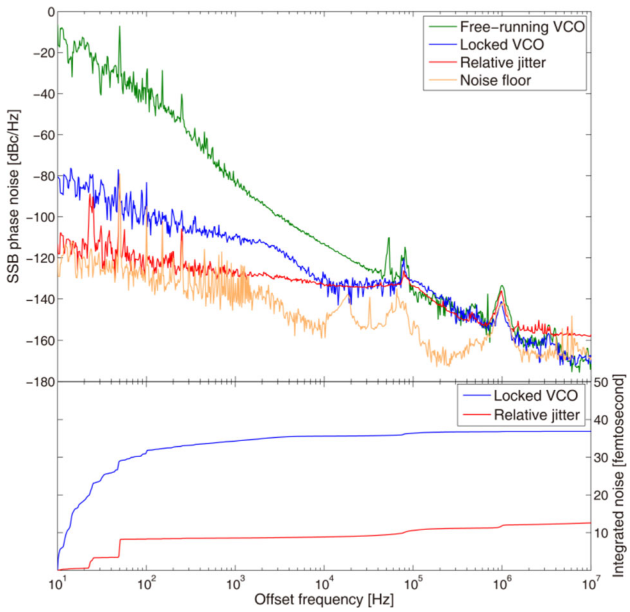

Fig. 5 (Color online) (Top) Single-sideband phase noise and (bottom) integrated noise (10 Hz–10 MHz)

2.856 GHz signal generated from an RF reference source can be divided into two signals by a 1:2 power divider. The noise floor is then obtained by measuring the relative timing jitter of these two 2.856 GHz signals originated from one source by the out-of-loop measurements setup. It should be noted that a phase shifter is inserted to adjust one signal's phase to assure the phases of the two signals are orthogonal in the mixer-based phase detector of the out-of-loop measurements setup.

The repetition rate of the mode-locked Er-fiber laser is locked to a RF reference source that is used as an external RF clock. As a result, the phase noise of the mode-locked Er-fiber laser below 1 kHz follows the phase noise of the RF reference source. The locked VCO phase noise follows the phase noise of the fiber laser within 50 kHz of the locking bandwidth, but follows the free-running VCO phase noise beyond the locking bandwidth. Low phase noise at the high offset frequency is the important characteristic of a VCO. We therefore exploit this trait to avoid transferring the phase noise of the mode-locked lasers to the high offset frequency by the photoelectric conversion. Some noise spurs from 50 Hz power frequency interference are present, including the 50 Hz power frequency and its harmonics in the 50–400 Hz range. It is important to note that the locking bandwidth is adjustable. The 50 kHz locking bandwidth is selected to minimize the relative jitter.

In a pass-band from 10 Hz to 10 MHz at the locked status, the in-loop timing jitter is as low as 34 fs (see Fig. 5(bottom)). The relative timing jitter between the extracted 2.856 GHz microwave signal and the input optical pulse is 16 fs at the same frequency offset range. The noise floor of the out-of-loop measurement setup is 9.3 fs. In order to optimize the total jitter of this scheme, the higher performance VCO will be used to reduce the noise floor. Other methods are also planned for improving the SNR of BOMPD detection, such as compressing pulse broadening using DCF, maintaining the phase using a PM fiber, eliminating 50 Hz power interference etc.

3 Conclusion and outlooks

We have proposed and demonstrated a novel RF signal extraction scheme from an optical pulse train. It has been experimentally demonstrated that the synchronization precision between an extracted 2.856 GHz microwave signal and a 238 MHz optical pulse train could reach sub-100 fs (10 Hz–10 MHz). An absolute timing jitter 34 fs and a relative timing jitter of 16 fs with a 50 kHz locking bandwidth were achieved using a BOMPD-based 3 × 3 coupler. The jitter of this device at high frequencies is limited by the performance of the VCO, and that at low frequencies is limited by the noise floor of the BOMPD. It was confirmed that a BOMPD based on a 3 × 3 coupler could meet the optical–RF synchronization requirements for SXFEL on the campus of SSRF. In the near future, the ultimate jitter performance will be improved by minimizing the noise floor using higher performance VCO, further suppression of pulse broadening and the elimination of 50 Hz power interference.

References

1. B.W.J. McNeil, N.R. Thompson, X-ray free-electron lasers. Nat. Photonics **4**, 814–821 (2010). https://doi.org/10.1038/nphoton.2010.239
2. W. Ackermann, G. Asova, V. Ayvazyan et al., Operation of a free-electron laser from the extreme ultraviolet to the water window. Nat. Photonics **1**, 336–342 (2007). https://doi.org/10.1038/nphoton.2007.76
3. T. Shintake, H. Tanaka, T. Hara et al., A compact free-electron laser for generating coherent radiation in the extreme ultraviolet region. Nat. Photonics **2**, 555–559 (2008). https://doi.org/10.1038/nphoton.2008.134
4. P. Emma, R. Akre, J. Arthur et al., First lasing and operation of an ångstrom-wavelength free-electron laser. Nat. Photonics **4**, 641–647 (2010). https://doi.org/10.1038/nphoton.2010.176
5. L. Redecke, K. Nass, D.P. DePonte et al., Natively inhibited *Trypanosoma brucei* cathepsin B structure determined by using an X-ray laser. Science **339**, 227–230 (2012). https://doi.org/10.1126/science.1229663
6. H.N. Chapman, P. Fromme, A. Barty et al., Femtosecond X-ray protein nanocrystallography. Nature **470**, 73–77 (2011). https://doi.org/10.1038/nature09750

7. S.M. Vinko, O. Ciricosta, B.I. Cho et al., Creation and diagnosis of a solid-density plasma with an X-ray free-electron laser. Nature **482**, 59–62 (2012). https://doi.org/10.1038/nature10746
8. B. Rudek, S. Son, L. Foucar et al., Ultra-efficient ionization of heavy atoms by intense X-ray free-electron laser pulses. Nat. Photonics **6**, 858–865 (2012). https://doi.org/10.1038/nphoton.2012.261
9. A. Rudenko, L. Inhester, K. Hanasaki et al., Femtosecond response of polyatomic molecules to ultra-intense hard X-rays. Nature **546**, 129–132 (2017). https://doi.org/10.1038/nature22373
10. N. Rohringer, D. Ryan, R.A. London et al., Atomic inner-shell X-ray laser at 1.46 nanometers pumped by an X-ray free-electron laser. Nature **481**, 488–491 (2012). https://doi.org/10.1038/nature10721
11. S. Bernitt, G.V. Brown, J.K. Rudolph et al., An unexpectedly low oscillator strength as the origin of the Fe XVII emission problem. Nature **492**, 225–228 (2012). https://doi.org/10.1038/nature11627
12. A. Azima, S. Düsterer, P. Radcliffe et al., Time-resolved pump-probe experiments beyond the jitter limitations at FLASH. Appl. Phys. Lett. **94**, 144102 (2009). https://doi.org/10.1063/1.3111789
13. M.B. Danailov, F. Bencivenga, F. Capotondi et al., Towards jitter-free pump-probe measurements at seeded free electron laser facilities. Opt. Express **22**, 12869–12879 (2014). https://doi.org/10.1364/OE.22.012869
14. J.M. Glownia, J. Cryan, J. Andreasson et al., Time-resolved pump-probe experiments at the LCLS. Opt. Express **18**, 17620–17630 (2010). https://doi.org/10.1364/OE.18.017620
15. J.H. Tan, Q. Gu, W.C. Fang, X-band deflecting cavity design for ultra-short bunch length measurement of SXFEL at SINAP. Nucl. Sci. Tech. **25**, 060101 (2014). https://doi.org/10.13538/j.1001-8042/nst.25.060101
16. E.N. Ivanov, S.A. Diddams, L. Hollberg, Analysis of noise mechanisms limiting the frequency stability of microwave signals generated with a femtosecond laser. IEEE J. Sel. Top. Quantum Electon. **9**, 1059–1065 (2003). https://doi.org/10.1109/jstqe.2003.819093
17. J. Kim, Y. Song, Ultralow-noise mode-locked fiber lasers and frequency combs: principles, status, and applications. Adv. Opt. Photonics **8**(3), 465–540 (2016). https://doi.org/10.1364/AOP.8.000465
18. A. Bartels, S.A. Diddams, T.M. Ramond et al., Modelocked laser pulse trains with sub-femtosecond timing jitter synchronized to an optical reference oscillator. Opt. Lett. **28**, 663–665 (2003). https://doi.org/10.1364/OL.28.000663
19. J. Kim, J. Chen, J. Coxe et al., Attosecond-resolution timing jitter characterization of free-running mode-locked lasers. Opt. Lett. **32**(24), 3519–3521 (2007). https://doi.org/10.1364/OL.32.003519
20. B. Lorbeer, F. Ludwig, H. Schlarb et al., Noise and drift characterization of direct laser to RF conversion scheme for the laser based synchronization system for FLASH at DESY, in *PAC. IEEE* (2007), p. 9861752. https://doi.org/10.1109/pac.2007.4440152
21. J. Kim, F.X. Kärtner, F. Ludwig, Balanced optical-microwave phase detectors for optoelectronic phase-locked loops. Opt. Lett. **31**, 3659–3661 (2006). https://doi.org/10.1364/OL.31.003659
22. B. Culshaw, The optical fibre Sagnac interferometer: an overview of its principles and applications. Meas. Sci. Technol. **17**, R1–R16 (2006). https://doi.org/10.1088/0957-0233/17/1/R01
23. J. Kim, F. Ludwig, M. Felber et al., Long-term stable microwave signal extraction from mode-locked lasers. Opt. Lett. **22**, 27102–27111 (2014). https://doi.org/10.1364/OE.22.027102
24. K. Jung, J. Kim, Subfemtosecond synchronization of microwave oscillators with mode-locked Er-fiber lasers. Opt. Lett. **37**, 2958–2960 (2012). https://doi.org/10.1364/OL.37.002958
25. W.Y. Zhang, B. Liu, X.Q. Liu et al., A balanced optical microwave regeneration system[p], Chinese patent: ZL201410455842.6 (2014)
26. H.X. Deng, Feasibility study on optical vortex generation at Shanghai deep ultraviolet free-electron laser. Nucl. Sci. Tech. **25**, 010101 (2014). https://doi.org/10.13538/j.1001-8042/nst.25.010101